Fabrication of Dissolving Polymer Microneedles for Controlled Drug Encapsulation and Delivery: Bubble and Pedestal Microneedle Designs

LEONARD Y. CHU,[1] SEONG-O CHOI,[2,3] MARK R. PRAUSNITZ[1,3]

[1]Wallace Coulter Department of Biomedical Engineering, Georgia Institute of Technology, Atlanta, Georgia 30332

[2]School of Electrical and Computer Engineering, Georgia Institute of Technology, Atlanta, Georgia 30332

[3]School of Chemical and Biomolecular Engineering, Georgia Institute of Technology, Atlanta, Georgia 30332

Received 19 November 2009; accepted 11 February 2010

Published online 5 April 2010 in Wiley Online Library (wileyonlinelibrary.com). DOI 10.1002/jps.22140

ABSTRACT: Dissolving microneedle patches offer promise as a simple, minimally invasive method of drug and vaccine delivery to the skin that avoids the need for hypodermic needles. However, it can be difficult to control the amount and localization of drug within microneedles. In this study, we developed novel microneedle designs to improve control of drug encapsulation and delivery using dissolving microneedles by (i) localizing drug in the microneedle tip, (ii) increasing the amount of drug loaded in microneedles while minimizing wastage, and (iii) inserting microneedles more fully into the skin. Localization of our model drug, sulforhodamine B in the microneedle tip by either casting a highly concentrated polymer solution as the needle matrix or incorporating an air bubble at the base of the microneedle achieved approximately 80% delivery within 10 min compared to 20% delivery achieved by the microneedles encapsulating nonlocalized drug. As another approach, a pedestal was introduced to elevate each microneedle for more complete insertion into the skin and to increase its drug loading capacity by threefold from 0.018 to 0.053 μL per needle. Altogether, these novel microneedle designs provide a new set of tools to fabricate dissolving polymer microneedles with improved control over drug encapsulation, loading, and delivery. J Pharm Sci 99:4228–4238, 2010

Keywords: transdermal drug delivery; dissolving microneedles; microneedle fabrication; drug encapsulation; skin

INTRODUCTION

Transdermal delivery as an alternative route to parenteral administration has gained increasing attention. A number of different transdermal patches delivering molecules less than approximately 500 Da and high lipophilicity such as nicotine, fentanyl and estrogen have been introduced commercially with significant clinical impact.[1] However, delivering biologics in the form of proteins or whole microorganisms across intact skin is extremely difficult due to the presence of stratum corneum, that is, the outer most layer of the skin. To overcome this skin barrier, microneedles offer a minimally invasive method that disrupts the stratum corneum in a relatively painless way.[2–4] Skin offers an excellent site for drug and vaccine delivery partly because delivering molecules via the skin bypasses intestinal and hepatic first-pass metabolisms. Moreover, the abundant presence of dendritic cells and Langerhans cells also makes skin an attractive site for vaccine delivery. Numerous studies have shown that the delivery of vaccines to the skin using intradermal injection or other methods that overcome the stratum corneum barrier effectively triggered immune response in animal models.[5,6]

Ideally, a skin delivery system should (i) deliver a broad range of therapeutics including small molecule drugs, macromolecules and biologics, (ii) have a controlled dose with high bioavailability, (iii) be safe, (iv) be simple to use, and (v) be inexpensive. Traditional non-invasive transdermal patch systems are simple to use and inexpensive, but the choice of therapeutics is limited to small molecules due to the presence of stratum corneum. In some cases, chemical enhancers have been used to facilitate the transport of molecules across the skin, but skin irritation can be a limitation.[7,8] Other approaches have included supramolecular structures, such as liposomes and

Correspondence to: Mark R. Prausnitz (Telephone: 404-894-5135: Fax: 404-894-2291; E-mail: prausnitz@gatech.edu)

Journal of Pharmaceutical Sciences, Vol. 99, 4228–4238 (2010)

emulsions, as well as physical approaches, such as iontophoresis, ultrasound, and thermal ablation.[9,10] However, each method has shortcomings and has made only limited clinical impact to date.

Recently, microneedles have shown the capability of delivering a variety of molecules into the skin, including drugs and vaccines.[11–19] Microneedles are micron-scale needles that are produced by adapting the tools of the microelectronics industry and pierce across the stratum corneum and into the epidermis and/or superficial dermis to administer compounds into the skin for local or systemic administration. Microneedles can be assembled into patches, which offers simplicity of use and low cost similar to conventional transdermal patches. Studies have shown that coated microneedles can carry a controlled dose by coating the drug only onto a defined region on the needle substrate surface.[14,15,20] The coated drug is released from the microneedle upon insertion into the skin. A drawback of this approach, however, is that such microneedles leave behind sharp, biohazardous waste after use, which may present safety concerns and special disposal needs.

Dissolving polymer needles have been developed by making microneedles out of water-soluble polymer that encapsulates drug within the needle matrix and fully dissolves upon insertion into the skin, thereby eliminating sharp biohazardous waste.[12,13,21–23] Thus, dissolving microneedles appear to be an attractive drug delivery system, because they are designed to deliver a wide range of therapeutics, are easy to use, are inexpensive, and leave no sharp waste after use. However, it can be difficult to control the dose encapsulated and delivered from polymer microneedles due in part to drug diffusion within the water-soluble microneedle matrix during fabrication.

This study seeks to improve upon dissolving microneedle design by better controlling drug encapsulation and delivery. More specifically, we seek to overcome the difficulties of controlling, loading, and delivering a specified drug dose with dissolving microneedles using novel approaches that (i) localize drug only in the microneedle tip, (ii) increase the amount of drug loaded in microneedles while minimizing wastage, and (iii) insert microneedles more fully into the skin. To localize drug only in the microneedle tip, we prevented drug diffusion out of microneedles during fabrication by either using a highly concentrated polymer solution to increase viscosity or introducing an air bubble at the base of the needle that constrained the drug from diffusing into the backing. To increase the amount of drug loaded in microneedles while minimizing wastage, we added a pedestal at the base of the microneedle to provide extra volume to each microneedle, thereby increasing their overall drug loading capacity. Finally, to insert microneedles more fully into the skin, we again used the pedestal design to provide higher aspect-ratio microneedles capable of inserting more fully into the skin and with sufficient mechanical strength to avoid failure during insertion.

MATERIALS AND METHODS

Fabrication of Microneedles

Microneedle Molds

Pyramidal Microneedle Mold. A mold of a 10×10 array of 300 μm $\times$ 300 μm $\times$ 600 μm ($W \times L \times H$) pyramidal microneedles with tip-to-tip spacing of 640 μm was fabricated using photolithography and molding techniques described previously.[24,25] Briefly, a pyramidal microneedle mold was created by exposing SU-8 photoresist (SU-8 2025, Microchem, Newton, MA) to ultraviolet light. A microneedle master structure made out of polydimethylsiloxane (PDMS) (Sylgard 184, Dow Corning, Midland, MI) was molded off the SU-8 mold and coated with gold. Next, a PDMS mold replicate was created from the gold-coated master structure. Then, polylactic acid (PLA) (L-PLA, 1.0 dL/g; DURECT, Pelham, AL) was melted at 195°C under vacuum to fill the mold replicate and make a PLA master structure replicate. Finally, a PDMS mold replicate was made from the PLA master structure replicate.

Pedestal Microneedle Mold. A pedestal microneedle mold was made by aligning a PDMS microneedle mold containing a 10×10 array of 300 μm $\times$ 300 μm $\times$ 600 μm (W $\times$ L $\times$ H) pyramidal cavities with two laser-cut stainless steel sheets each containing a 10×10 array of 340 μm $\times$ 340 μm $\times$ 150 μm ($W \times L \times H$) non-tapered through-holes. The pattern of the non-tapered through-holes was first drafted in AutoCAD software (Autodesk, Cupertino, CA) and then cut into 150 μm stainless steel sheets (McMaster-Carr, Atlanta, GA) using an infrared laser (Resonetics Maestro, Nashua, NH) at a cutting velocity of 1 mm/s with 20% attenuation of laser energy. The laser-cut metal sheets were electropolished (E399 electropolisher, ESMA, South Holland, IL) for 10 min at 2 A in a 74°C mixture of glycerin, 85% ortho-phosphoric acid and water (6:3:1 by volume) (Fisher Scientific, Fair Lawn, NJ). The electropolished metal sheets were washed briefly with 30% nitric acid solution at room temperature and blow-dried with nitrogen gas. Individual metal arrays patterned with 10×10 through-holes were detached from their mother electropolished metal sheet. Each metal array was then coated with a thin PDMS film by spin coating at 672*g* for 1 min (GS-15R, Beckman, Fullerton, CA). Two 150 μm-thick metal arrays coated with PDMS were aligned and stacked on top of the PDMS mold.

An integrated metal-PDMS composite mold was formed as the PDMS coating adhered the metal sheets and PDMS mold together upon curing at 150°C for 10 min.

Extended Pyramidal Microneedle Mold. The extended pyramidal microneedle master structure was made by trimming off the sides of the 340 μm × 340 μm × 300 μm pedestal to form a structure with an extended microneedle base of 300 μm × 300 μm × 300 μm ($W \times L \times H$) using a razor blade. Polyvinyl alcohol (PVA) (MW 2000, ACROS Organics, Geel, Belgium) was dissolved in DI water (50 wt%) and was used to smooth the rough surfaces of the tapered needle structure. The viscous polymer solution was applied as a coating onto the tapered microneedle structure by centrifuging at 3200*g* at 25°C for 1 h. After the polymer coating was centrifuge-dried, the extended pyramidal microneedle mold was made by curing the PDMS on top of the extended microneedle structure with a PVA coating at 37°C overnight.

Preparation of Microneedle Matrix Material

The microneedle matrix material was a polymer blend consisting of polyvinyl alcohol (PVA) (MW 2000, ACROS Organics, Geel, Belgium) and polyvinylpyrrolidone (PVP) (BASF, K17, Aktiengesellschaft, Ludwigshafen, Germany) (ratio 3:1). To make a 50 wt% polymer solution, 3 g PVA was dispersed in 4 mL DI water and heated at 60°C for 3 h. Then, 1 g PVP was then added to the PVA solution and mixed thoroughly using a spatula. The polymer blend was incubated at 37°C in a sealed glass bottle overnight. Similarly, 30 and 40 wt% polymer solutions were also prepared. Unless indicated, a 50 wt% polymer solution was used to fabricate the microneedles. Viscosity of the polymer solutions was measured using a rheometer at 25°C (Physica MCR 300, Paar Physica USA, Inc., Ashland, VA).

Drug Loading into the Mold

Sulforhodamine B (MW 559 Da, Molecular Probes, Eugene, OR) is a water-soluble, non-fixative red-fluorescent dye with excitation/emission peaks of 565/586 nm. It was used as the model drug and was dissolved in DI water to prepare stock solutions at concentrations of 1 and 10 mg/mL. Two methods of drug loading were used for different studies. The first method was a two-step process that first loaded and dried the drug solution in the mold cavities and then cast the polymer solution into the mold. This method created a drug gradient in which the tip of the microneedle had the highest concentration. Sulforhodamine B stock solution was pipetted onto the top of a PDMS mold to cover the cavities and then was vacuumed at room temperature to −91 kPa for 3 min. After vacuuming, residual sulforhodamine B on the mold surface was pipetted off and recycled for reuse. The PDMS mold filled with sulforhodamine B was then dried under centrifugation at 3200*g* at room temperature for several minutes. Dried sulforhodamine B adherent to the mold surface was removed by Scotch tape (3 M, St. Paul, MN). The second method involved the direct casting and drying of a pre-mixed drug and polymer solution, as described below. In this case, the drug was uniformly distributed within the microneedle matrix upon drying. This method was used to quantify the dissolution of microneedles based on the amount of drug released into the skin.

Polymer Casting into the Mold

Approximately 150 μL PVA/PVP blend solution was applied to cover the entire array of microneedle cavities in the mold. The mold covered with polymer solution was vacuumed at room temperature to −91 kPa for 5 min. To fabricate solid microneedles, the residual polymer (30 and 40 wt%) on the mold surface was left to dry at room temperature. When 50 wt% polymer was used, low-speed centrifugation (168*g*) was applied to accelerate the drying process. To make bubble microneedles, the residual polymer (30 and 40 wt%) was spun off by centrifuging at 3200*g* at room temperature for 5 min and then dried at room temperature. Because it was difficult to remove more viscous 50 wt% polymer (having a viscosity of 6350 cP) from the mold surface, the residual polymer was manually scrapped off the mold surface instead.

Backing Assembly

The backing layer was assembled differently for solid and bubble microneedles. To assemble the backing for bubble microneedles, a small piece of office paper (approx. 1 cm × 1 cm) was coated with a thin film of a highly concentrated PVA/PVP solution and placed on top of the mold after polymer casting and drying in an ambient air environment. The assembled mold was then dried at room temperature over night. For solid needles, no additional backing assembly was done, because the residual polymer left on the mold surface was used as the backing after drying. In both cases, after the microneedles and backing were both dried, the resulting microneedle array was detached from the mold using double-sided adhesive tape (444 Double-Sided Polyester Film Tape, 3 M). The microneedle array was then attached to a SEM mount (Structure Probe, West Chester, PA), which served as the handle to facilitate manual handling and insertion into the skin.

In Vitro Microneedle Insertion Assessment

Microneedle Insertion into Skin

Excised porcine skin (Pel-Freez, Rogers, AR) was shaved using a razor (Dynarex, Orangeburg, NY).

The skin's subcutaneous fat was removed by a scalpel (Feather, Osaka, Japan). The processed skin was laid flat on a cutting board at room temperature. The surface of the skin was dried with a paper towel. Microneedles were manually inserted into the skin while positioning two fingers on either side of the intended insertion site to keep it under mild tension. These microneedles were inserted by pushing against the skin at a distance of approximately 1 cm from the skin surface. Pyramidal, extended pyramidal and pedestal microneedles containing sulforhodamine B were each manually inserted into the skin for 30 s, 2 min and 10 min. Each subset of microneedles for each insertion time had 3 replicates. The microneedles were microscopically imaged before and after insertion (Olympus SZX16, Pittsburgh, PA).

Imaging and Histology

The microneedle insertion sites were excised from the bulk skin with a scalpel. The isolated skin pieces were placed in cryostat molds embedded in optimum cutting temperature (OCT) media (Tissue-Tek, Torrance, CA). The skin was fixed in OCT by freezing the sample on dry ice. Frozen skin samples were sliced into 12-μm thick sections (Cryo-star HM 560 MV, Microm, Waldorf, Germany). The skin sections were stained with hematoxylin and eosin using an automated staining machine (Leica Autostainer XL, Nussloch, Germany). After staining, the sections were covered with glass slides sealed with cytoseal 60 (low viscosity, Richard-Allan Scientific, Kalamazoo, MI). The sections were dried overnight before taking images under the microscope (Nikon E600, Tokyo, Japan).

Bioavailability

Spectrofluorometer. The amount of drug delivered into the skin was determined based on a mass balance of three parameters: the total amount of drug encapsulated in microneedles before insertion into skin, the amount of drug remaining in needles after insertion and removal from skin, and the residual drug left on the skin surface. The samples for the total amount of sulforhodamine B encapsulated in microneedles were prepared by dissolving the microneedles containing sulforhodamine B before insertion in DI water for 30 min at room temperature. In contrast, the samples for the residual drug left on the skin surface were obtained by a single tape-stripping (3 M, St. Paul, MN) of the skin surface to remove the residual dye left on the skin surface after the needles were removed from the insertion site. Both the inserted microneedles and skin-stripped tapes were then soaked in DI water in separate containers for 30 min at room temperature. These samples were transferred into cuvettes and measured by spectrofluorometry (Photon Technology International, Lawrenceville, NJ). The excitation wavelength of sulforhodamine B was set at 565 nm. Area under the curve from 580 to 620 nm was calculated using Felix software (Photon Technology International). This reading was fitted into the sulforhodamine B standard curve to obtain the actual amount of sulforhodamine B by mass. The amount of sulforhodamine B delivered into the skin was determined by subtracting the amount of sulforhodamine B left in the needles and on the skin surface from the amount originally encapsulated in the microneedles.

RESULTS

Microneedle Fabrication

In this study, we introduce new fabrication processes to better control drug encapsulation within dissolving microneedles. Microneedles with pyramidal geometry were fabricated by a series of molding and casting techniques. In this process, drug was loaded selectively into the microneedles (i.e., and not in the backing). We did not want to spread the drug solution to cover the entire microneedle mold and then dry it because this method could result in non-uniform drug loading or large amounts of drug wastage in the backing. Instead, we loaded the drug into the microneedle cavities of the mold (Fig. 1A) and then recycled the residual drug solution on the mold surface using pipettes to avoid wastage (Fig. 1B). To keep the drug localized in the microneedle cavities of the mold, we evaporated the drug solution to leave a solid drug film in the tips of the mold cavities prior to casting the polymer solution (Fig. 1C and D).

We next formed the microneedle base and backing using different methods to produce microneedles of two different designs: solid microneedles and bubble microneedles. Solid needles were made by casting sufficient polymer solution to form the microneedle base and backing after drying (Fig. 1E1). The dried microneedles were then peeled off from the mold (Fig. 1F1). To make bubble needles, the polymer solution outside the mold cavities was spun off the mold surface. Upon drying, the polymer solution in the mold cavities solidified with a meniscus-like shape in each microneedle cavity (Fig. 1E2). Upon applying a second layer of polymer solution to the mold surface, surface tension effects prevented it from filling the empty space in the mold cavities defined by the polymer meniscus. After drying, this left a void—that is, a bubble—between the backing layer and the microneedles (Fig. 1F2).

Using this fabrication approach, the maximum amount of drug loaded into each microneedle is the product of the microneedle cavity volume times the drug solubility in its carrier solvent. One approach to

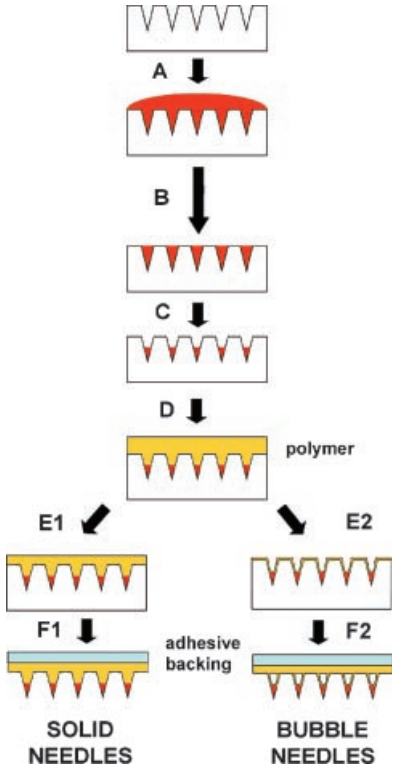

Figure 1. Schematic of solid and bubble needle fabrication process. A: A PDMS microneedle mold was filled with drug solution under vacuum. B: Residual drug solution was removed from the surface by a pipette and later reused. C: Drug solution in the mold cavities was dried under centrifugation. D: Drug-free polymer solution was cast onto the mold and filled under vacuum. E1: The polymer solution was either air-dried or dried under centrifugation at low speeds. F1: Dried solid needles were peeled off the mold by an adhesive backing. E2: The polymer solution was either physically scraped off the mold surface and then air-dried or dried under centrifugation at high speeds. F2: A backing coated with a thin film of concentrated polymer solution was placed on top of the mold and then air dried. After drying, the bubble needles were peeled off.

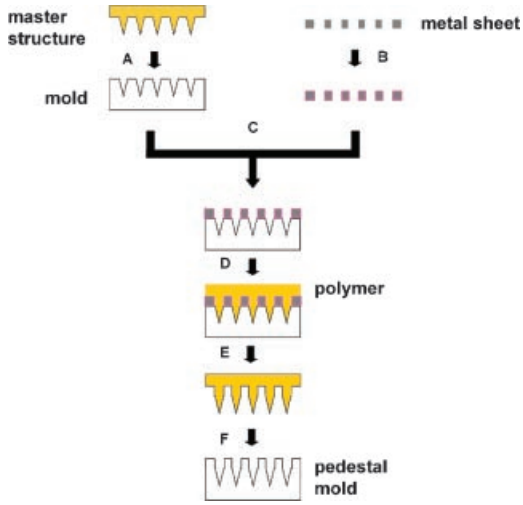

Figure 2. Schematic of pedestal microneedle mold fabrication. A: A PDMS mold was created from a master microneedle structure. B: An infrared laser-cut metal sheet was coated with PDMS. C: A composite mold was formed as the coated metal sheet(s) were placed on top of the PDMS mold and cured under heat. D: Molten polymer was cast onto the composite mold by vacuum. E: After cooling, microneedles with pedestal structure were peeled off the composite mold. F: The pedestal microneedles were then used as the master structure for making pedestal PDMS mold replicates (see Fig. 1).

increase drug loading per microneedle would be to use a solvent that increases drug solubility, although choice of solvents is also limited by safety considerations. Another possibility would be to overcome the solubility limit by using particulate systems in which drug particles are suspended in the carrier solvent. However, particle size must be much smaller than microneedle size and such systems can lead to nonuniform needle-to-needle loading. As another alternative, we increased loading capacity of microneedles by effectively increasing microneedle mold cavity volume by adding a pedestal at the base of each mold cavity. To accomplish this, the pyramidal PDMS mold was reverse-molded from a master microneedle needle structure (Fig. 2A). We then aligned PDMS-coated laser-cut stainless steel sheets with the PDMS mold (Fig. 2B and C). In this way, each pyramidal cavity in the mold was positioned immediately below a hole in the stacked metal sheets above. This created enlarged microneedle mold cavities consisting of a nontapered pedestal at the base of the pyramidal needle tip. Extended pyramidal microneedles and pedestal microneedles were then fabricated in a manner similar to above (Fig. 2E and F).

Drug Localization and Delivery Efficiency

One of our goals was to develop methods to load and localize drug in the tips of the microneedles. To study the drug localization and delivery efficiency, we loaded the pyramidal microneedle molds with 1 mg/mL sulforhodamine B. Using the solid microneedles, we found that polymer concentration in the casting solution had an important effect. As shown in Figure 3A, using a low concentration casting solution (30 wt%, 98 cP) led to distribution of the model drug, sulforhodamine B, throughout the needle and into the backing. We believe that the low viscosity of the low concentration casting solution allowed sulforhodamine B to diffuse out of the microneedle mold cavity through the microneedle matrix during drying in the microneedle mold. Consistent with this hypothesis, increasing viscosity by increasing the polymer concentration (40 wt%, 557 cP) better kept the sulforhodamine B within the needle (Fig. 3B). Casting at a still higher polymer concentration (50 wt%, 6350 cP)

 DOI 10.1002/jps

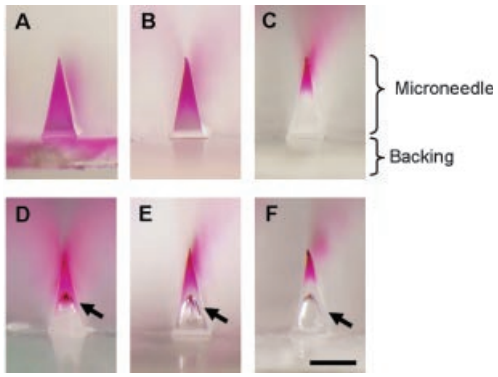

Figure 3. Solid and bubble microneedles loaded with model drug (appearing pink) localized to the tips imaged by bright field microscopy. Top row: Solid needles loaded with 1 mg/mL sulforhodamine B encapsulated in (A) 30 wt%; (B) 40 wt%; (C) 50 wt% PVA/PVP blends. Bottom row: Bubble needle counterparts loaded with 1 mg/mL sulforhodamine B encapsulated in (D) 30 wt%; (E) 40 wt%; (F) 50 wt% PVA/PVP blends. The arrows indicate the location of air bubbles. Bar = 300 μm.

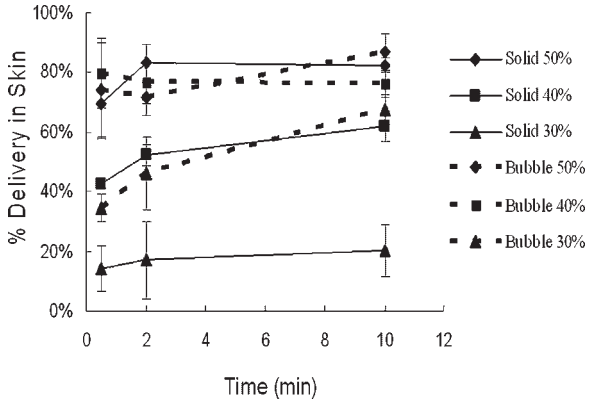

Figure 4. Percentage delivery of sulforhodamine B over the time during microneedle insertion into excised porcine skin. Solid lines are for solid microneedles and dashed lines are for bubble microneedles made using different polymer concentration solutions. Data points represent averages of $n = 3$ replications, with standard deviation bars shown.

localized the sulforhodamine B even more to the microneedle tip (Fig. 3C).

Because microneedle formulations are subject to many constraints such that sufficiently increasing casting solution viscosity may be problematic, we developed another approach to keeping drug in the microneedle tip by introducing an air bubble at the base of the microneedle. Using this approach, sulforhodamine B was contained within the microneedle independent of polymer concentration (Fig. 3D–F). We believe this was because the bubble formed a physical barrier that prevented diffusion out of the microneedle. As an aside, the bubble also decreased the mechanical strength of the microneedles, which could be a limitation in some situations. However, under the conditions used in this study we found that bubble microneedles inserted reliably into skin and did not ever break (i.e., based on the data reported here, as well as additional experiments involving on the order of 100 microneedle insertions in the context of other studies (data not shown)).

We were motivated to keep sulforhodamine B localized in the tips of the microneedles because we expected that to enable more efficient drug delivery into the skin (i.e., leaving less drug remaining in the microneedle device). To test this expectation, we inserted solid and bubble microneedles made using different polymer concentrations into excised porcine skin and monitored drug release over time. As shown in Figure 4, delivery efficiency was highly correlated with drug localization. Microneedles with drug localized in the microneedle tip (i.e., Solid 50%, Bubble 50%, and Bubble 40%) showed an initial burst release of sulforhodamine B within the first 30 s resulting in approximately 80% drug release within 10 min. Microneedles with sulforhodamine B distributed throughout the needle matrix but not in the backing (i.e., Solid 40% and Bubble 30%) had a smaller burst release, but then delivery efficiency increased over time to approximately 70% drug release, probably due to continued microneedle matrix dissolution. Finally, microneedles with sulforhodamine B distributed into the backing demonstrated low delivery efficiency corresponding to only about 20% drug release. The delivery did not significantly increase with time, suggested that 10 min was insufficient time for the sulforhodamine B in the backing to diffuse into the skin, and was therefore wasted.

Drug Loading Capacity and Variability

Our second goal was to increase drug loading in the microneedles without wastage in the backing. To achieve a higher loading in the microneedles, we made larger microneedle mold cavities, which enabled more drug solution to be cast into each cavity and resulted in larger microneedles. We did not change the tip geometry, because it is critical to microneedle insertion into the skin. Instead we elongated the base portion of the needle either in a tapered fashion, which resulted in "extended pyramidal" microneedles or with a nontapered structure, which generated "pedestal" microneedles. The original pyramidal needle has a volume of 18 nL. Elongating the base in the extended pyramidal needle increased the volume to 45 nL, which is two and a half times larger than the pyramidal needle. The pedestal microneedle volume was increased to 53 nL, which is almost three times larger than the pyramidal needle. As an example, casting with a solution containing 10 mg/mL of drug results in 0.53 μg of drug encapsulated per

Table 1. Drug Loading Using Three Different Microneedle Designs ($n \geq 3$)

	Pyramidal		Extended Pyramidal		Pedestal	
Microneedle mold cavity volume (per 100 microneedles)	1.80 μL		4.50 μL		5.30 μL	
Drug concentration in the loading solution	1 mg/mL	10 mg/mL	1 mg/mL	10 mg/mL	1 mg/mL	10 mg/mL
Drug loaded after encapsulation (per 100 microneedles)	1.33 ± 0.1 μg	18.10 ± 0.74 μg	4.16 ± 0.45 μg	40.55 ± 0.62 μg	6.37 ± 0.44 μg	54.30 ± 0.92 μg
Drug wastage during fabrication (per 100 microneedles)	0.11 ± 0.09 μg	1.13 ± 0.29 μg	0.19 ± 0.03 μg	1.36 ± 0.63 μg	0.08 ± 0.1 μg	1.28 ± 0.3 μg

needle (i.e., 53 μg in 100 needles or 530 μg in 1000 needles). These doses are sufficient for many vaccines and protein therapeutics.[26,27]

We made measurements of drug loading dose to assess reproducibility and wastage ($n \geq 3$). As shown in Table 1, the amount of sulforhodamine B encapsulated within microneedles was determined at two different drug concentrations in the casting solution and using the three different microneedle designs. We found that the amount encapsulated within the microneedles was close to that predicted as the product of microneedle mold cavity volume times drug concentration, although there was some deviation especially when lower drug concentration was used. The device-to-device variability ranged from 0.1 μg to 0.92 μg per 100 microneedles on an absolute basis, which corresponded to 8% and 2% respectively on a percent basis.

Drug wastage, as assessed by the amount of drug left on the mold surface (i.e., not inside a mold cavity), scaled with drug concentration and was relatively independent of mold geometry. Wastage ranged from 0.08 μg to 0.19 μg when casting with 1 mg/mL sulforhodamine B and from 1.13 to 1.36 μg when casting at 10 mg/mL. This corresponds to a residual volume on the mold surface on the order of 100 nL per 100-needle array. Because the absolute wastage amount was relatively independent of mold geometry, drug wastage was just 5% and 3% respectively for the extended pyramid needles and 1% and 2% respectively for the pedestal needles. We expect that these values could be further reduced with additional optimization and automation of the protocol.

Microneedle Insertion Depth

Our third goal was to achieve a more complete insertion of microneedles into the skin. We hypothesized that by inserting microneedles more fully would result in higher drug bioavailability in the skin. The extended pyramid and pedestal microneedles achieved greater drug loading by elongating the needle base, which makes the needles longer. Because skin deflection during microneedle insertion can result in a significant fraction of the needle remaining outside the skin,[23,28] the original pyramidal microneedles are not expected to fully insert. However, mounting them on a pedestal or on an elongated based should facilitate full insertion of the microneedle tip, in which the drug is encapsulated. Clearly, there is a limit to how far this strategy can be carried forward. Still longer microneedles should encapsulate more drug and insert more fully into the skin. However, if the microneedles become too big, then they will hurt, which could reduce patient acceptance.

To study this issue, pyramidal microneedles, extended pyramidal microneedles and pedestal microneedles were fabricated as shown in Figure 5A, B, and C. The pyramidal microneedles were 600 μm long and the extended pyramidal and pedestal needles were 900 μm long. We determined the depth of microneedle insertion and its impact on the amount of drug delivered to the skin in three ways. First, we examined the histological cross sections of skin at the insertion sites. As shown in the representative images in Figure 5A1, B1, and C1, pyramidal microneedles inserted to a depth of approximately

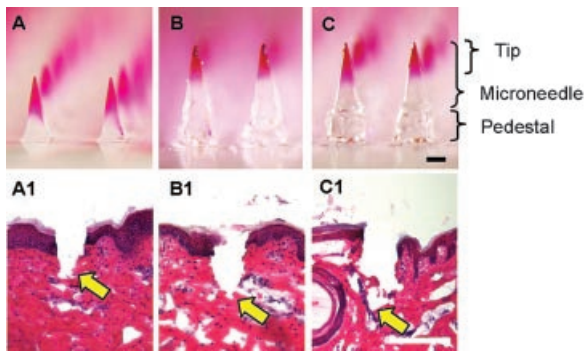

Figure 5. Skin insertion depth of three different microneedle structures imaged by brightfield microscopy. A: Pyramidal microneedles (base width × base depth × needle height: 300 μm × 300 μm × 600 μm). B: Extended pyramidal microneedles (300 μm × 300 μm × 900 μm). C: Pedestal microneedles (340 μm × 340 μm × 900 μm). Corresponding H&E-stained histology cross sectional images of insertion sites in excised porcine skin: (A1) Pyramidal microneedles; (B1) Extended pyramidal microneedles and (C1) Pedestal microneedles. The arrows indicate the depth of the microneedle insertion track. Bar = 200 μm.

 DOI 10.1002/jps

150 μm, whereas both the extended pyramidal and pedestal needles inserted to a depth of approximately 250 μm into the excised porcine skin, which was similar to 250 μm length of the drug-loaded tip portion of the needles. Although the pedestal needles had a bulkier base than the extended pyramidal needles, the pedestal did not appear to hamper insertion, perhaps because the base portion of the microneedle was primarily used to overcome skin deflection and did not insert into the skin itself.

As a second assessment, we determined how the insertion depth affected the dissolution of the microneedles. As determined by microscopic examination of needles after 2 min insertion, we found that pyramidal needles lost approximately 50% of their original length from 600 to 300 μm (Fig. 6A and A1). Because of the tapered geometry, this corresponds to a 12.5% loss in microneedle volume. In contrast, both the extended pyramidal needles and pedestal needles lost almost 80% of their microneedle tips, reducing from 600 μm to approximately 150 μm (Fig. 6B, B1, and C, C1). This corresponds to complete dissolution of the upper 450 μm containing the drug-loaded tip.

Third, we further determined the amount of delivery by quantifying the efficiency of microneedle insertion and dissolution in the skin based on the amount of encapsulated drug released during the insertion. To facilitate this analysis, we encapsulated the model drug, sulforhodamine B, uniformly throughout the microneedle by premixing the drug and the microneedle matrix polymer solution rather than localizing it in the tips. A mass balance on the amount of sulforhodamine B initially encapsulated and that remaining after insertion showed that the pyramidal needles lost approximately 10% of their original volume, where as both the extended pyramidal and pedestal needles lost almost 50% of their microneedle matrix (Fig. 7). Altogether, these three methods of assessment reach the common conclusion that the elongated microneedle geometries enable a deeper insertion and more efficient delivery of drug into the skin.

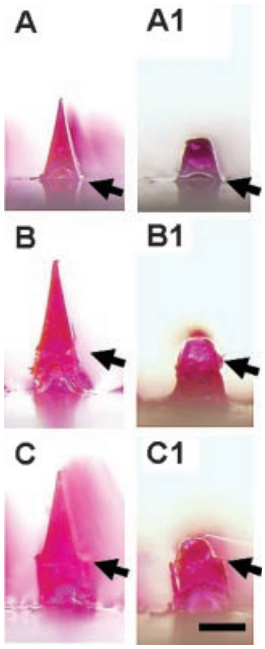

Figure 6. Microneedle dissolution after insertion into excised porcine skin imaged by bright field microscopy. Left column shows microneedles uniformly loaded with 1 mg/mL sulforhodamine B before insertion into skin. A: Pyramidal microneedle, (B) extended pyramidal microneedle, (C) pedestal microneedle. Right column shows corresponding microneedles after a 2 min insertion into skin. The arrows indicate the base of the primary 600 μm microneedle structure at its interface with the extended pyramidal portion or pedestal portion. Bar = 300 μm.

DISCUSSION

Dissolving polymer microneedles offer a simple, safe, and minimally invasive delivery method to the skin. Yet, due to the need for water-based casting of the polymer when molding the needles, drug encapsulation, loading and delivery can be difficult to control. We addressed these issues by (1) localizing drug only in the microneedle tip, (2) increasing the amount of drug loaded in microneedles while minimizing wastage, and (3) inserting microneedles more fully into the skin.

Localizing drug only in the microneedle tip required control of drug deposition in the tip during casting as well as minimizing drug diffusion out of the tip during drying. When the drug and polymer matrix material were premixed and cast onto the microneedle mold together, the volume of this mixture would take up too much space in the microneedle

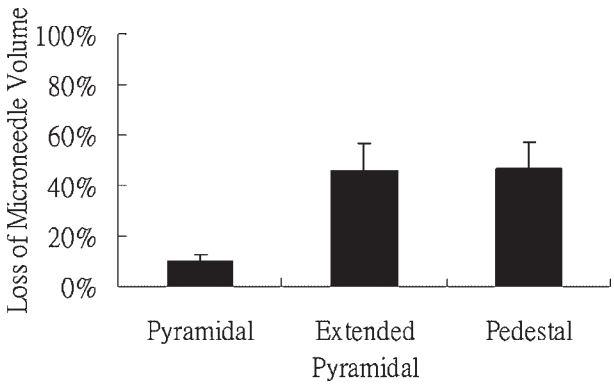

Figure 7. Microneedle dissolution after insertion into excised porcine skin as determined by a quantitative mass balance. Loss of microneedle volume was determined based on the amount of sulforhodamine B encapsulated in microneedles before and after insertion in skin for 2 min. Data points represent averages of $n = 3$ replications, with standard deviation bars shown.

mold upon drying and thereby make localization in the microneedle tip difficult. In this study, we showed that drug localization in the tip can be better achieved by first casting a solution containing drug with little or no added excipients and then drying the drug into the tip of the microneedle mold under centrifugal force. As a second step, this was followed by casting and drying the polymer solution to form the rest of the microneedle matrix.

During this second step, diffusion of drug out of the tip can take place as the dried drug makes contact with, dissolves in and diffuses through the aqueous polymer solution. As shown in Figure 3, drug diffusion during this step is affected by polymer concentration, such that a higher concentration solution inhibited diffusion and helped maintain drug localization in the tip. However, use of highly concentrated polymer solutions can be constrained by their physical characteristics including high viscosity, poor solubility or gelation, which can make processing during fabrication difficult.

As an alternative to blocking diffusion through the use of concentrated polymer solutions, we introduced a new technique in which dilute polymer solution could be used and drug diffusion from the tip was blocked by incorporating a bubble at the base of each microneedle. In this approach, the excess polymer was spun off the mold surface and, after drying, a concave drug film was formed in the base of each microneedle mold cavity, as shown in Figure 1E2. Instead of refilling the hollowed cavity, which could re-dissolve the drug, the hollow cavity was left unfilled and capped with a backing layer containing little moisture. The outcome of this technique was an entrapped air bubble that blocked drug diffusion. Comparing the bubble needles with their solid needle counterparts, the bubble needles had more defined drug localization even in microneedles made up of dilute polymer solutions. Moreover, microneedles with better drug localization showed greater delivery efficiency compared to the ones with less effective drug localization.

In addition to localizing drug into the microneedle tip, we also sought to maximize the dose encapsulated in a microneedle while avoiding the wastage of drug. Any drug that dried on the mold surface was considered wasted because it could not be recycled or delivered into the skin easily. To minimize drug wastage, we only loaded drug solutions in the microneedle mold cavities, which resulted in the dose encapsulated per needle being constrained by the volume of the needle itself. To address this limitation, we modified the pyramidal needles by introducing two additional structures: extended pyramidal needles and pedestal needles. These new microneedle structures bulked up the original pyramidal needle volume from 0.018 to 0.045 and 0.053 μL respectively. The amount of drug wastage was independent of the microneedle structure. Rather, the wastage was determined by the amount of unrecycled drug left on the mold surface. As a result, encapsulating larger doses was preferred because the relative percent wastage of drug became less significant as we increased the dose (Tab. 1).

Skin deflection and elasticity is one of the main causes for incomplete insertion of microneedles. The degree of skin deflection depends on a variety of factors including microneedle tip sharpness, microneedle aspect ratio, needle-to-needle spacing, microneedle length and insertion speed. Because the matrix of dissolving polymer microneedles is weaker (i.e., has a smaller Young's modulus) than, for example, metal microneedles, dissolving microneedle geometry must provide added mechanical strength, which usually results in a wide needle (i.e., smaller aspect ratio). This geometry makes dissolving microneedles more difficult to insert fully into the skin compared to, for example, the slender, high-aspect ratio metal needles used in other studies.[14,29–31]

As the needles are inserted into the skin, the insertion stops as the deflected skin surface hits the backing of the needle array, which prevents the needles from further piercing. To reduce the impact of this issue, we elevated the microneedles by adding a pedestal to the base of the microneedle. According to Figure 5, we found that the additional 300 μm offered by the pedestal only resulted in an additional 100 μm insertion depth. This may be because the pedestal only partially overcame the skin deflection without the presence of physiological skin tension in our *in vitro* apparatus. In principle, needle length could be extended longer, but in practice, it would be difficult to remove dissolving microneedles longer than 1 mm from the PDMS mold and pain caused by such long needles may become a concern.[32]

Controlled dosing administered by dissolving microneedles plays a critical role in their eventual use in medicine. Some compounds such as biotherapeutics and vaccines are relatively expensive to produce. A controlled drug encapsulation process with minimal wastage reduces the overall cost of a microneedle patch, especially for costly drugs. In some cases, when a drug has a narrow therapeutic window, controlled dosing becomes crucial to avoid over-or under-dosing. Another important aspect of this study is the more complete insertion of microneedles. People in different age groups and in different weight categories have different skin mechanical properties. The ability to insert microneedles more fully into the skin reduces the likelihood of delivery failure due to variable skin types. Overall, the new fabrication techniques introduced here bring dissolving polymer microneedle technology closer to practical use.

CONCLUSIONS

We have introduced new methods to fabricate dissolving microneedles for controlled drug encapsulation and delivery. These new microneedle designs and drug loading techniques enabled more drug to be loaded and localized into the microneedle tip with minimal drug wastage. By increasing polymer concentration in the casting solution or incorporating a bubble into the base of the microneedles, drug was encapsulated more effectively in the microneedle tip. By incorporating a pedestal at the base of the microneedle, microneedles could insert more fully. More complete insertion of the microneedles allowed a higher fraction of the encapsulated drug to be delivered into the skin due to more rapid and complete needle dissolution. Overall, these technical advancements of controlled encapsulation and delivery provide an important step toward developing dissolving microneedles to serve as a reliable, versatile and safe delivery tool for administering a wide range of therapeutics.

ACKNOWLEDGMENTS

We thank Dr. Mark Allen for the use of the IR laser in his lab and Mr. Richard Shafer for IR training and maintenance. We also thank Dr. Victor Breedveld for the use of the rheometer in his lab and Mr. Kayode Olanrewaju for the viscosity measurements. This work was supported in part by the National Institutes of Health. The work was carried out in the Center for Drug Design, Development and Delivery, and the Institute for Bioengineering and Bioscience at the Georgia Institute of Technology. M.R.P. serves as a consultant and is an inventor on patents licensed to companies developing microneedle-based products. This possible conflict of interest has been disclosed and is being managed by Georgia Tech and Emory University.

REFERENCES

1. Prausnitz MR, Langer R. 2008. Transdermal drug delivery. Nat Biotech 26:1261–1268.
2. Prausnitz MR. 2004. Microneedles for transdermal drug delivery. Adv Drug Deliv Rev 56:581–587.
3. Prausnitz MR, Gill HS, Park JH. 2008. Microneedles for drug delivery. 2nd edition. New York: Informa Healthcare. p. 295–309.
4. Sivamani RK, Liepmann D, Malbach HI. 2007. Microneedles and transdermal applications. Expert Opin Drug Deliv 4:19–25.
5. Glenn GM, Kenney RT, Ellingsworth LR, Frech SA, Hammond SA, Zoeteweij JP. 2003. Transcutaneous immunization and immunostimulant strategies: Capitalizing on the immunocompetence of the skin. Expert Rev Vaccines 2:253–267.
6. Glenn GM, Taylor DN, Li X, Frankel S, Montemarano A, Alving CR. 2000. Transcutaneous immunization: A human vaccine delivery strategy using a patch. Nat Med 6:1403–1406.
7. William AC, Barry BW. 2004. Penetration enhancers. Adv Drug Deliv Rev 56:603–618.
8. Karande P, Jain A, Ergun K, Kispersky V, Mitragotri S. 2005. Design principles of chemical penetration enhancers for transdermal drug delivery. Proc Natl Acad Sci 102:4688–4693.
9. Arora A, Prausnitz MR, Mitragotri S. 2008. Micro-scale devices for transdermal drug delivery. Int J Pharm 364:227–236.
10. Sinico C, Fadda AM. 2009. Vesicular carriers for dermal drug delivery. Expert Opin Drug Deliv 6:813–825.
11. Wermeling DP, Banks SL, Hudson DA, Gill HS, Gupta J, Prausnitz MR, Stinchcomb AL. 2007. Microneedles permit transdermal delivery of a skin-impermeant medication to humans. Proc Natl Acad Sci 105:2058–2063.
12. Kolli CS, Banga AK. 2007. Characterization of solid maltose microneedles and their use for transdermal delivery. Pharm Res 25:104–113.
13. Ito Y, Yoshimitsu JI, Shiroyama K, Sugioka N, Takada K. 2006. Self-dissolving microneedles for the percutaneous absorption of EPO in mice. J Drug Target 14:255–261.
14. Gill H, Prausnitz MR. 2007. Coated microneedles for transdermal delivery. J Control Release 117:227–237.
15. Cormier M, Johnson B, Ameri M, Nyam K, Libiran L, Zhang DD, Daddona P. 2004. Transdermal delivery of desmopressin using a coated microneedle array patch system. J Control Release 97:503–511.
16. Chabri F, Bouris K, Jones T, Barrow D, Hann A, Allender C, Brain K, Birchall J. 2004. Microfabricated silicon microneedles for nonviral cutaneous gene delivery. Br J Dermatol 150:869–877.
17. Mikszta JA, Dekker JP III, Harvey NG, Dean CH, Brittingham JM, Huang J, Sullivan VJ, Dyas B, Roy CJ, Ulrich RG. 2006. Microneedle-based Intradermal delivery of the anthrax recombinant protective antigen vaccine. Infect Immun 74:6806–6810.
18. Gardeniers HJGE, Luttge R, Berenschot EJW, de Boer MJ, Yeshurun SY, Hefetz M, van't Oever R, van den Berg A. 2003. Silicon micromachined hollow microneedles for transdermal liquid transport. J Microelectromech Syst 12:855–862.
19. Verbaan FJ, Bal SM, van den Berg DJ, Groenink WHH, Verpoorten H, Luttge R, Bouwstra JA. 2007. Assembled microneedle arrays enhance the transport of compounds varying over a large range of molecular weight across human dermatomed skin. J Control Release 117:238–245.
20. Zhu Q, Zarnitsyn VG, Ye L, Wen Z, Gao Y, Pan L, Skountzou I, Gill HS, Prausnitz MR, Yang C, Compans RW. 2009. Immunization by vaccine-coated microneedle arrays protects against lethal influenza virus challenge. Proc Natl Acad Sci 106:7968–7973.
21. Sullivan SP, Murthy N, Prausnitz MR. 2008. Minimally invasive protein delivery with rapidly dissolving polymer microneedles. Adv Mater 20:933–938.
22. Miyano T, Tobinga Y, Kanno T, Matsuzaki Y, Takeda H, Wakui M, Hanada K. 2005. Sugar micro needles as transdermic drug delivery system. Biomed Microdevices 7:185–188.
23. Lee JW, Park JH, Prausnitz MR. 2007. Dissolving microneedles for transdermal drug delivery. Biomaterials 29:2113–2124.
24. Park JH, Yoon YK, Choi SO, Prausnitz MR, Allen MG. 2007. Tapered conical polymer microneedles fabricated using an integrated lens technique for transdermal drug delivery. IEEE Trans Biomed Eng 54:903–913.
25. Choi SO, Rajaraman S, Yoon YK, Wu X, Allen MG. 2006. 3-D Metal patterned microstructure using inclined UV exposure

and metal transfer micromolding technology. Solid-State Sensor, Actuator, and Microsystems Workshop.
26. Gorse GJ, Keefer MC, Belshe RB, Matthews TJ, Forrest BD, Hsieh RH, Koff WC, Hanson CV, Dolin R, Weinhold KJ, Frey SE, Ketter N, Fast PE. 1996. A dose-ranging study of a prototype synthetic HIV-1MN V3 branched peptide vaccine. The National Institute of Allergy and Infectious Diseases AIDS Vaccine Evaluation Group. J Infect Dis 173:330–339.
27. Keitel WA, Atmar RL, Cate TR, Petersen NJ, Greenberg SB, Ruben F, Couch RB. 2006. Safety of high doses of influenza vaccine and effect on antibody responses in elderly persons. Arch Intern Med 166:1121–1127.
28. Martanto W, Moore JS, Couse T, Prausnitz MR. 2006. Mechanism of fluid infusion during microneedle insertion and retraction. J Control Release 112:357–361.
29. Park JH, Allen MG, Prausnitz MR. 2005. Biodegradable polymer microneedles: Fabrication, mechanics and transdermal drug delivery. J Control Release 104:51–66.
30. Davidson A, Al-Qallaf B, Das DB. 2008. Transdermal drug delivery by coated microneedles: Geometry effects on effective skin thickness and drug permeability. Chem Eng Res Des 86: 1196–1206.
31. Widera G, Johnson J, Kim L, Libiran L, Nyam K, Daddona PE, Cormier M. 2006. Effect of delivery parameters on immunization to ovalbumin following intracutaneous administration by a coated microneedle array patch system. Vaccine 24:1653–1664.
32. Gill HS, Denson DD, Burris BA, Prausnitz MR. 2008. Effect of microneedle design on pain in human volunteers. Clin J Pain 24:585–594.